

TWO-PHASE MODELS OF FORMATION OF CAVITATING SPALLS IN A LIQUID

M. N. Davydov and V. K. Kedrinskii

UDC 532.5.013.2+532.528+534.222

The dynamics of the structure of a liquid layer structure (with microbubbles of a free gas) behind a rarefaction wave front is studied numerically using the two-phase Iordansky–Kogarko–van Wijngaarden model and the “frozen” mass-velocity field model. An analysis of the initial stage of cavitation by the Iordansky–Kogarko–van Wijngaarden model showed that tensile stresses behind the rarefaction wave front relax quickly and the mass-velocity field in the cavitation zone turns out to be “frozen.” This effect is used to describe the late stage of the development of the cavitation zone. These models were combined to study the formation of cavitating spalls in a free-surface liquid under shock-wave loading.

Key words: liquid strength, dynamic loading, bubble cavitation, spalls.

Introduction. It is well-known that the strength of liquids under dynamic loading is a less definite and concrete notion than the strength of solids under deformation. This is mainly due to the fact that real liquids contain microheterogeneities, namely, free gas microbubbles, solid microparticles, or their combinations [1–4]. For example, it has been found experimentally that the density of microbubbles in a volume of distilled water is on the order of 10^4 cm^{-3} per unit volume and their characteristic size is $1.5 \text{ }\mu\text{m}$; the total density of microparticles is approximately 10^6 cm^{-3} (the maximum on the particle-size distribution curve is at $0.8 \text{ }\mu\text{m}$ [5]). As estimates of [1, 3–5] show, the volume fraction of microheterogeneities ranges from 10^{-8} to 10^{-12} . These microparticles act as cavitation nuclei. In solids, failure starts with defect nucleation [6], whereas in liquids, structural defects already exist in the form of cavitation nuclei. This fact explains why the theoretical strength of real liquids (of the order of 10^4 atm) cannot be attained experimentally. We also might assume that a liquid in this state has properties of a heterogeneous medium.

The presence of cavitation nuclei with that low volume content do not affect the propagation of shock waves over a liquid. The situation changes dramatically if the liquid is subjected to tensile stresses (rarefaction phases or waves). Under the action of the latter, the nuclei begin to expand to form a zone of bubble cavitation with a rapidly increasing vapor–gas phase, whose volume fraction changes by five to six orders of magnitude in fractions of a microsecond if the rarefaction-wave amplitudes reach several hundred atmospheres. Experiments show that this process can be divided into the following several stages: formation and growth of bubble clusters, unlimited bubble growth in clusters until the formation of a foam, decomposition of the foam to form cavitating fragments, and transition of the medium into a gas–droplet state [7]. This process was defined as the process of inversion of the two-phase state of the medium, which involves cavitation breakup of a real free-surface liquid, in particular, formation of cavitating spalls, under explosive loading of the liquid [8]. Spalling phenomena indicate that a cavitating liquid can have properties of a fragile solid with a characteristic spall-layer thickness of about several millimeters (Fig. 1).

1. Initial Stage of Cavitation (Iordansky–Kogarko–van Wijngaarden Model). Based on the above data on microheterogeneities in real liquids, a liquid can be treated as a two-phase structure and the dynamics of development of the cavitation zone and the structure of tensile stresses in it can be described by a corresponding mathematical model [9]. From the viewpoint of physics, of special interest is the Iordansky–Kogarko–van Wijn-

Lavrent'ev Institute of Hydrodynamics, Siberian Division, Russian Academy of Sciences, Novosibirsk 630090. Translated from *Prikladnaya Mekhanika i Tekhnicheskaya Fizika*, Vol. 44, No. 5, pp. 71–78, September–October, 2003. Original article submitted March 31, 2003.

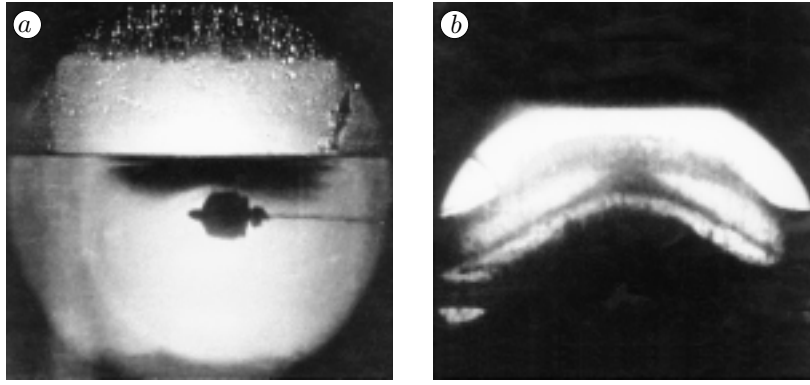


Fig. 1. Bubble cavitation zone (a) and two cavitating spalls (b) in an underwater explosion near the free surface.

gaarden model (IKW model) [10–12], which includes the conservation laws of gas dynamics for average pressures, mass velocities, and densities, the system of equations that relates the average density and the gas-phase volume fraction via the bubble radius, and the Rayleigh equation:

$$\begin{aligned} \frac{d\rho}{dt} + \rho \operatorname{div} \mathbf{u} = 0, \quad \frac{d\mathbf{u}}{dt} + \frac{\nabla p}{\rho} = 0, \quad \rho = (1 - k)\rho_l, \quad k = k_0 \left(\frac{R}{R_0}\right)^3, \\ p = B \left[\left(\frac{\rho}{\rho_0}\right)^n - 1 \right], \quad R \frac{d^2 R}{dt^2} + \frac{3}{2} \left(\frac{dR}{dt}\right)^2 = \rho_l^{-1} (p_g - p), \quad p_g = p_0 \left(\frac{R_0}{R}\right)^{3\gamma}. \end{aligned}$$

Use of this model to calculate the rarefaction-wave parameters in the cavitation zone generated by these waves promoted the discovery of the following two fundamental phenomena: for rarefaction waves with intensities of hundreds of atmospheres propagating in a real liquid with microheterogeneities, the relaxation times are on the order of 1 μsec and the steepness of the rarefaction wave fronts determines the maximum tensile stresses admitted by a cavitating liquid [13]. Since the experimental characteristic time of cavitation development is at least tens of microseconds for the indicated tensile stress values, it can be concluded that tensile stresses are totally absorbed in a developed cavitation zone and that the weak nonuniform pressure field in this zone can be replaced by a constant pressure field, for example, a hydrostatic one. Taking into account the law of conservation of momentum, it is easy to see that the mass velocity profile must be “frozen” in the cavitation zone. This conclusion was supported by experimental studies of the dynamics of mass velocities in cavitation zones on samples of distilled water in a hydrodynamic shock tunnel using special labeling and flash radiography [14]. The results obtained have led to the development of a new approach to studying cavitation — the model of a “frozen mass velocity field in a growing zone of bubble cavitation” [15–17].

Let us examine a wavy structure that appears upon reflection of a piston-generated ultrashort shock wave from the free surface of a thin (2 cm thick) layer of a real liquid within the classical hydrodynamic shock tunnel problem in a one-dimensional formulation. To formulate the problem, the system of gas-dynamic equations was written in Lagrangian coordinates as

$$\frac{\partial u}{\partial t} + \frac{1}{\rho_0} \frac{\partial p}{\partial r} = 0, \quad \frac{\partial x}{\partial t} = u, \quad \frac{1}{\rho} = \frac{\partial x}{\partial r},$$

where u is the mass velocity, x is an Eulerian coordinate, r is a Lagrangian coordinate, and p and ρ are the average pressure and density, respectively.

This system of equations is solved by an explicit differential scheme using linear and quadratic von Neumann–Richtmyer artificial viscosities and the method described in [18]. The value of the artificial viscosity are chosen such that the pressure oscillations behind the shock-wave front are smooth with retention of the front steepness.

Let at the time $t = 0$, the piston placed on the left side of the tunnel begins to move. This motion generates a shock pulse (curve 1 in Fig. 2) with an amplitude of 150 atm and a duration of 3 μsec in the liquid layer, which

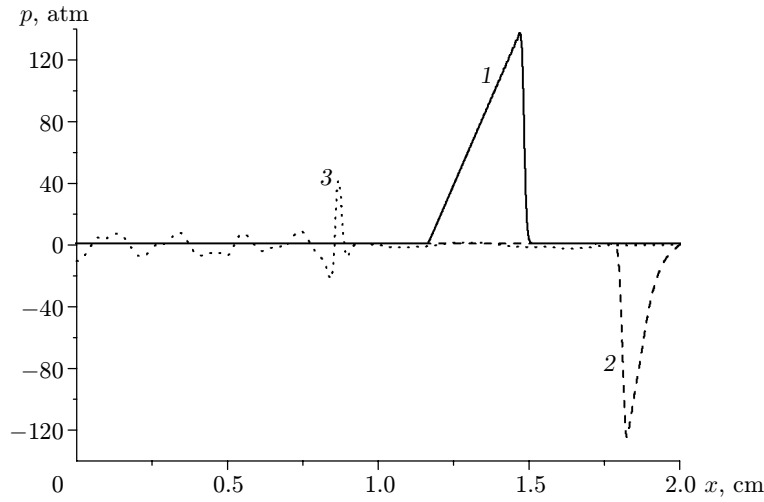


Fig. 2. Pressure profiles for $t = 9.7$ (1), 14.5 (2), and $32.4 \mu\text{sec}$ (3).

propagates to the right and is reflected from the free surface. According to experimental data, the liquid in a stable state contains free gas microbubbles of initial radius $R_0 \simeq 1.5 \cdot 10^{-4}$ cm (cavitation nuclei) and an initial gas-phase volume fraction of $k_0 \simeq 10^{-7}$. Calculations for the IKW model show that reflection of the shock pulse from the free surface gives rise to a rarefaction wave in the liquid layer (curve 2 in Fig. 2), which propagates into the layer depth, initiates growth of cavitation nuclei, and transforms into a wave “packet” with a system of positive and negative phases. The packet is five times wider than the initial shock pulse. The wave field formed determines the structure of the cavitation zone, which, by the time the wave packet is reflected from the solid piston ($t \simeq 27 \mu\text{sec}$), has been divided into separate zones, in each of which the bubble radius and volume fraction have different maximum values. At the time $t = 32.4 \mu\text{sec}$, the front of the wave packet reflected from the piston reaches the coordinate $x \simeq 1$ cm (curve 3 in Fig. 2). As follows from calculations for the other half of the layer ($x \simeq 1-2$ cm), which is not perturbed by the reflected wave, the relaxation of tensile stresses has virtually been completed (Fig. 2) and the use of the “frozen” mass velocity condition is justified.

2. Development of Cavitation in a “Frozen” Mass-Velocity Field. The model of a “frozen” field implies that the IKW model is used to calculate the dynamics of the mass velocity and pressure fields up to complete relaxation of tensile stresses in the cavitation zone. When the maximum amplitude of the tensile stresses reaches a specified “critical” value (for example, decreases by two orders of magnitude), the pressure field that has formed by that time is replaced by a uniform hydrostatic pressure field, whereas the velocity field is fixed and retained during further development of the zone.

With allowance for the aforesaid, the system of gas-dynamic equations is written as

$$\frac{\partial u}{\partial t} = 0, \quad \frac{\partial x}{\partial t} = u, \quad \frac{1}{\rho} = \frac{\partial x}{\partial r}, \quad p = p_0.$$

We note that unlike the IKW model, the “frozen” field approach has no limitation on the growth of the bubble volume fraction. In this case, the bubble volume fraction can grow without bound up to the value corresponding to the “bulk” density of the bubbles. Based on the calculation results under the above conditions, one can introduce the “freezing” condition for the mass velocity profile at the time $t_* = 33 \mu\text{sec}$. Figure 3 shows pressure and velocity profiles calculated for the IKW model before the transition (curves 1 and 3) and after the transition (curves 2 and 4). As can be seen, in the vicinity of the free surface there is a large velocity gradient on a “length” of 2.5 mm, which is slightly less than the length of the incident shock wave. We note that weak oscillations of the wave field amplitude, in fact, have no effect on the mass velocity profile, whose shape is almost identical for both models. Both profiles have an intermediate maximum, which plays an important role, as shown by further calculations.

It is of interest to compare another characteristics of the cavitation zone for the two models — the dynamics of the bubble volume fraction. Figure 4 shows calculation results for a certain point in the zone of intensely developing cavitation. The calculation results obtained for the IKW model and the “frozen” field model (the latter was included in calculations starting from $t = 33 \mu\text{sec}$, when the rarefaction wave amplitude in the cavitation zone

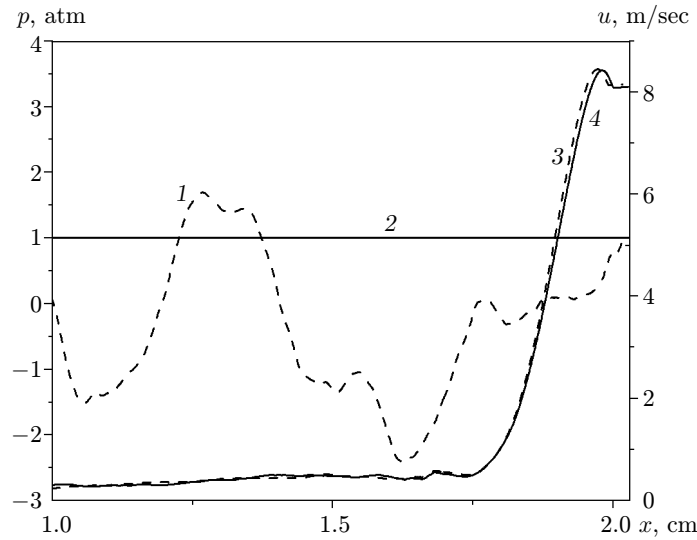


Fig. 3. Pressure profiles (1 and 2) and mass velocity profiles (3 and 4) for $t = 32.4$ (1 and 3) and $43 \mu\text{sec}$ (2 and 4).

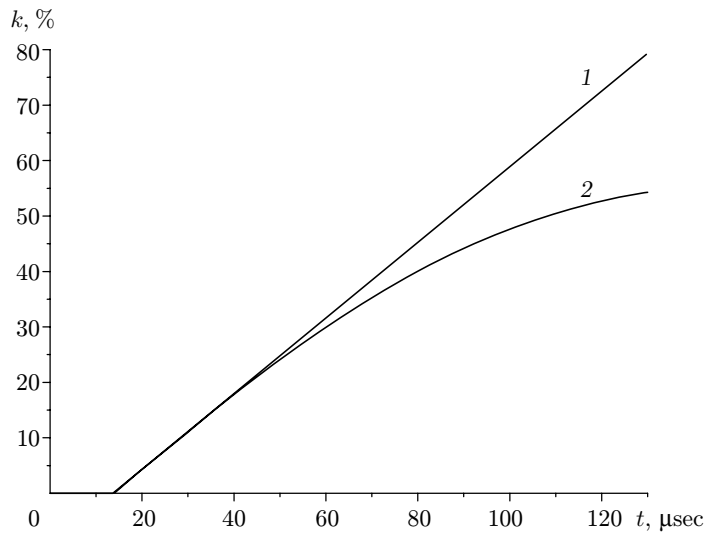


Fig. 4. Dynamics of the bubble volume fraction k in the cavitation zone: 1) calculations for the “frozen” field model; 2) calculations for the IKW model.

did not exceed 2% of the shock pulse amplitude) agree well until the times of 40–45 μsec . By this time, the volume fraction exceeds 20%, having increased by six to seven orders of magnitude, and the wave packet reflected from the piston reaches the free surface. We note that the difference becomes substantial after the entire cavitation zone is “perturbed” by the wave packet reflected from the piston.

As one might expect from calculations, cavitation develops most intensely in the vicinity of the free surface (Fig. 5). In this case, bubbles pulsate in some part of the zone. By $t = 53 \mu\text{sec}$, the bubbles collapse in a thin liquid layer adjacent to the free surface, and then they start growing to form an isolated cavitation layer, in which the bubble volume fraction in the time interval $t = 57\text{--}86 \mu\text{sec}$ increases to 15% (Fig. 5).

In the subsequent times, the volume fraction reaches the value corresponding to the “bulk” density of the bubbles (Fig. 6). The calculation results suggest that the further bubble merging will result in the formation of two cavitating spalling layers: a main layer 3 mm thick and a thin cavitating layer with a characteristic thickness of fractions of a millimeter (Fig. 6). We note that when the volume fraction in the main spalling layer reaches 80%, the free boundary is shifted by about 1.5 mm.

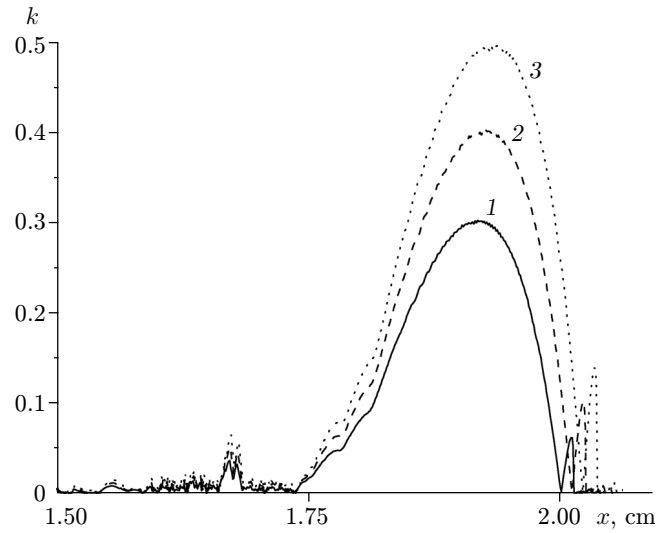


Fig. 5. Distribution of the bubble volume fraction over the x coordinate for $t = 57$ (1), 72 (2), and $86 \mu\text{sec}$ (3).

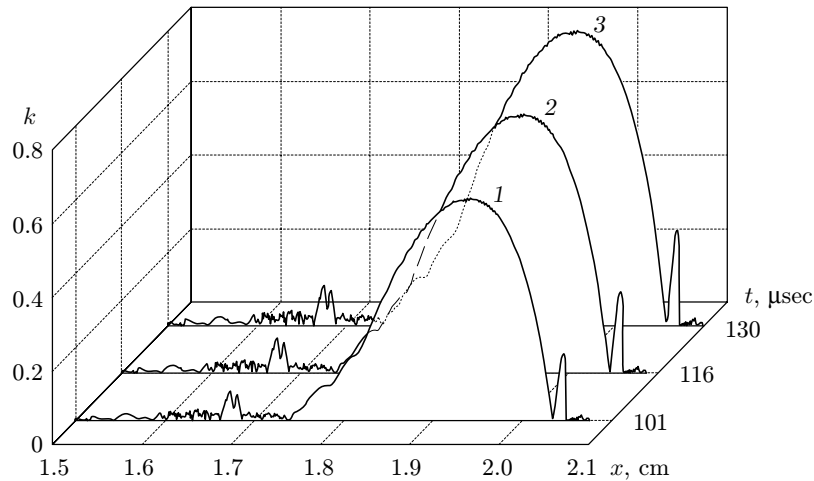


Fig. 6. Formation of cavitating spalls in the vicinity of the free surface of the liquid layer for $t = 101$ (1), 116 (2), and $130 \mu\text{sec}$ (3).

Calculations of the formation of cavitating spalling layers using a combination of the IKW model and the “frozen” mass velocity field model were also performed for an incident bell-shaped shock wave with an amplitude of 50 atm and a duration of $2 \mu\text{sec}$ propagating in a liquid layer 1 cm thick (see Fig. 7). In Fig. 7, curve 1 corresponds to the incident shock wave, curve 2 refers to the wave reflected from the free surface, and curve 3 is the pressure distribution in the layer at $t = 14.7 \mu\text{sec}$. The left side of the figure shows a wave packet reflected from the piston, whose front has reached the coordinate $x = 0.4$ cm. As in the case above, the pressure field ahead of the wave packet is virtually uniform up to the free surface in the cavitation zone, where the conditions of the “frozen” mass-velocity field can be introduced beginning from the indicated time. Our calculations show that in this formulation, the cavitation zone develops on a length of 2–3 mm near the free surface. The structure of this zone is shown in Fig. 8. It is evident that two cavitating spalling zones form in the layer. The zone that is the closest to the free surface develops more intensely than the second one.

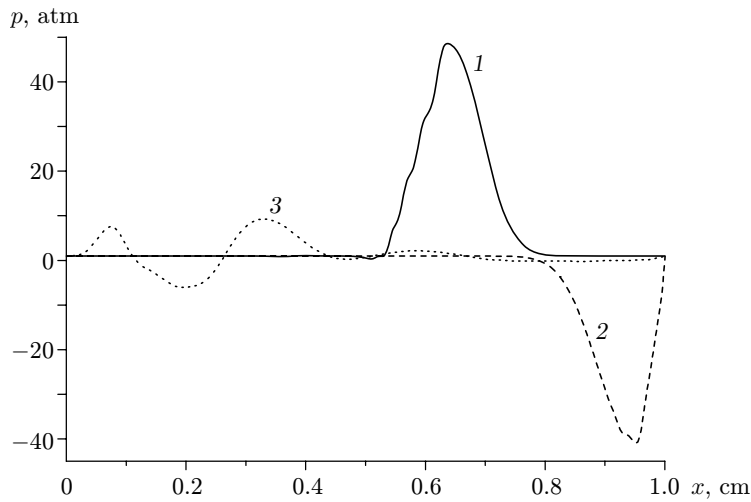


Fig. 7. Pressure profiles for $t = 4.6 \mu\text{sec}$ (1), 7.4 (2), and $14.7 \mu\text{sec}$ (3).

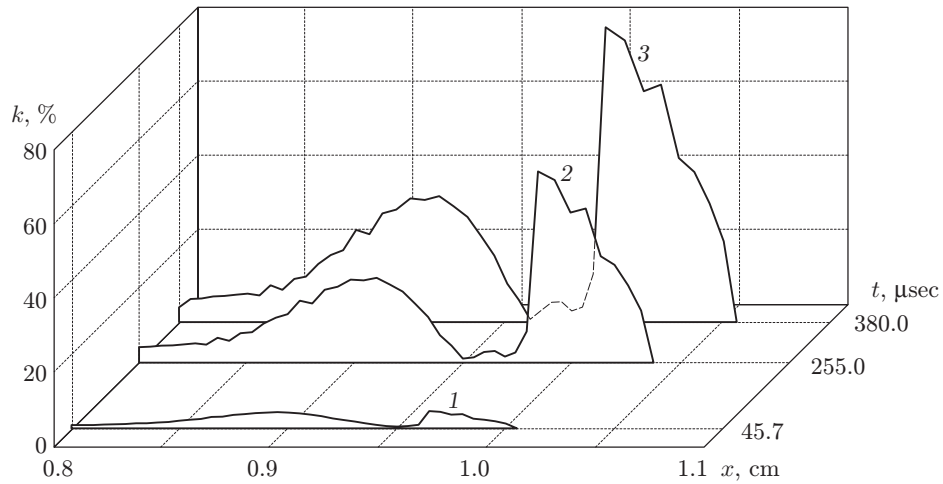


Fig. 8. Dynamics of formation of two spalling zones near the layer surface for $t = 45.7$ (1), 255 (2), and $380 \mu\text{sec}$ (3).

3. Conclusions. Using as an example the problem of the development of bubble cavitation in thin liquid layers with free gas microbubbles, it is shown that the experimentally justified combination of the IKW model and the “frozen” mass velocity field model can be used to calculate the formation of cavitating spalls in the liquid layer under shock-wave loading. These effects are presumably observed in viscous liquid media, such as magma, which undergoes phase transitions under the action of tensile stresses, for example, during volcanic eruptions. In such media, however, cavitation nuclei can also result from desorption of dissolved gases or melt crystallization. Furthermore, since the mass fraction of water dissolved in magma is considerable (more than 5%), cavitation effects can develop rapidly up to disruption of magma into fragments.

The work was supported by the INTAS Foundation (Grant No.) and the Russian Foundation Fundamental Research (Grant No. 03-01-00274).

REFERENCES

1. M. Strasberg, "Undissolved air cavities as cavitation nuclei," in: *Cavitation in Hydrodynamics*, Nat. Phys. Lab., London (1956), pp. 1–13.
2. F. S. Hammitt, A. Koller, and O. Ahmed, et al. "Cavitation threshold and superheat in various fluids," in: *Proc. of the Conf. on Cavitation* (Edinburgh, Sept. 3–5, 1974), Mech. Eng. Publ., London (1976), pp. 341–354.
3. A. S. Besov, V. K. Kedrinskii, and E. I. Pal'chikov, "Study of the initial stage of cavitation by a diffraction–optical method," *Pis'ma Zh. Tekh. Fiz.*, **10**, No. 4, 240–244 (1984).
4. R. L. Gavrilov, "Free-gas content in fluids and methods for measuring it," in: *Strong Ultrasonic Field* [in Russian], Vol. 4, Nauka, Moscow (1970).
5. V. K. Kedrinskii, "On relaxation of tensile stresses in cavitating liquid," in: *Proc. 13th Int. Congress on Acoustics* (Beograd, 1989), Vol. 1, Dragan Srnic Press, Sabac (1989), pp. 327–330.
6. L. D. Volovets, N. A. Zlatin, and G. S. Pugachev, "Nucleation and development of submicrocracks in polymethyl methacrylate under dynamic tension (spalling)," *Pis'ma Zh. Tekh. Fiz.*, **4**, No. 18, 1079–1084 (1978).
7. I. G. Getts and V. K. Kedrinskii, "Dynamics of explosive loading of a finite volume of a dense two-phase mixture," *J. Appl. Mech. Tech. Phys.*, No. 2, 280–284 (1989).
8. V. K. Kedrinskii, "The experimental research and hydrodynamical models of a "sultan," *Arch. Mech.*, **26**, Nos. 3/4, 535–540 (1974).
9. V. K. Kedrinskii, "Dynamics of the cavitation zone during an underwater explosion near the free surface," *J. Appl. Mech. Tech. Phys.*, No. 5, 724–733 (1975).
10. S. V. Iordanskii, "Equations of motion for a liquid containing gas bubbles," *Zh. Prikl. Mekh. Tekh. Fiz.*, No. 3, 102–110 (1960).
11. B. S. Kogarko, "A model of a cavitating liquid," *Dokl. Akad. Nauk SSSR*, **137**, No. 6, 1331–1333 (1961).
12. L. van Wijngaarden, "On the collective collapse of a large number of cavitation bubbles in water," in: *Proc. 11th Intern. Congress of Appl. Mech.* (Munich, Germany, August 1964), Springer-Verlag, Berlin (1964), pp. 854–861.
13. V. K. Kedrinskii, "Negative pressure profile in a cavitation zone at underwater explosion near a free surface," *Acta Astronaut.*, **3**, Nos. 7/8, 623–632 (1976).
14. V. K. Kedrinskii, A. R. Bergardt, and N. N. Chernobaev, "Behavior of a liquid under dynamic loading," in: *Proc. of the IUTAM Symp. on Waves in Liquid/Gas and Liquid/Vapour Two-Phase Systems* (Kyoto, Japan, May 9–13, 1994), Kluwer Acad. Publ., Dordrecht (1995), pp. 429–438.
15. N. N. Chernobaev, "Modeling of shock-wave loading of liquid volumes," in: *Proc. of the IUTAM Symp. on Adiabatic Waves in Liquid–Vapor Systems* (Göttingen, 1989), Springer-Verlag, Berlin (1989), pp. 361–370.
16. M. N. Davydov, "Development of cavitation in a drop under shock-wave loading," in: *Dynamics of Continuous Media* (collected scientific papers) [in Russian], No. 117, Novosibirsk (2001), pp. 17–20.
17. V. K. Kedrinskii, "Nonlinear problems of cavitation breakdown of liquids under explosive loading (review)," *J. Appl. Mech. Tech. Phys.*, **34**, No. 3, 361–377 (1993).
18. A. A. Samarskii and Yu. P. Popov, *Difference Methods for Solving Problems of Gas Dynamics* [in Russian], Nauka, Moscow (1980).